Influence of length of resonance tubes on multi-stage looped thermoacoustic electric generator

Tianjiao Bi [a,b], Zhanghua Wu [b,**], Limin Zhang [b], Jingyuan Xu [c], Ercang Luo [b], Chao Li [a], Bin Zhang [a], Wei Chen [a,*]

[a] College of Electromechanical Engineering, Qingdao University of Science and Technology, Qingdao 266061, China
[b] CAS Key Laboratory of Cryogenics, Technical Institute of Physics and Chemistry, CAS, Beijing 100190, China
[c] Mechanical and Electrical Engineering Division, Karlsruhe Institute of Technology, Karlsruhe 76344, Germany

Keywords:
Thermoacoustic
Resonance tube
Multi-stage looped thermoacoustic electric generator

A B S T R A C T

Resonance tubes are often used to connect multi-stage looped thermoacoustic heat engine and linear alternators to form a multi-stage looped thermoacoustic electric generator. In this paper, we experimentally investigate the performance of a multi-stage looped thermoacoustic electric generator with two sets of resonance tubes of different lengths. With the increase of the length of resonance tubes from 1.5 m to 2 m, the system frequency decreases from 70 Hz to 62 Hz. The maximum output acoustic power increases from 6.97 kW to 8.16 kW, and the maximum output electric power increases from 5.09 kW to 6.24 kW. Meanwhile, the maximum thermoacoustic efficiency increases from 23.08 % to 23.94 %, the maximum acoustic-to-electric efficiency increases from 78.03 % to 82.06 % and the maximum thermal-to-electric efficiency increases from 17.79 % to 19.64 %. Numerical simulation is also conducted based on a 3-step coupling method and validates the experimental results. This study demonstrates that adjusting the length of resonance tubes in a multi-stage looped thermoacoustic electric generator is an effective way to tune the frequency as well as to improve the coupling between the multi-stage looped thermoacoustic heat engine and linear alternators.

1. Introduction

Thermoacoustic is a subject that deals with the power conversion of thermal energy to acoustic power. In Nikolaus Rott's [1] review of thermoacoustic, the meaning of the word"thermoacoustic" is "rather self-explanatory", it is an interdisciplinary science that encompasses the fields of thermodynamics and acoustics [2]. After imposing a high enough temperature gradient on a porous media or stack that holds a compressible gas as the working substance, a spontaneous acoustic oscillation will be induced in the vicinity of the solid-gas interface. This is the basic principle of a thermoacoustic heat engine (TAHE). The spontaneous acoustic oscillation, which is often viewed as a form of acoustic power or mechanical power, can be used to drive an electric generator [3], thermoacoustic refrigerator (cryocooler) [4], and thermoacoustic heat pump [5].

In recent years, the concept of multi-stage looped TAHE has been popular. Since 2010 when the design strategy was first proposed by de Blok [6], it has been proven valid in multi-stage looped thermoacoustic electric generator (TAEG) [7], thermoacoustic refrigerator [8]and combined system [9]. The multi-stage looped TAHE concept is attractive in two aspects: Firstly, it can achieve relatively low onset temperature. Jin and Yang [10] have obtained the lowest heating temperature of 29 °C (corresponding onset temperature difference of 17 °C) in both 3-stage and 4-stage looped TAHE. Secondly, it can achieve relatively high output power. Bi and Wu have obtained the maximum acoustic power of 6.68 kW with thermoacoustic efficiency of 22.32 % in a 3-stage looped TAHE [11], and the maximum acoustic power of 8.16 kW with thermoacoustic efficiency of 21.18 % in a 4-stage looped TAHE [12]. The second reason makes the multi-stage looped TAHE a promising candidate for high-power TAEG after being connected with an appropriate acoustic-to-electric conversion device.

Due to the high acoustic-to-electric efficiency and stability of linear alternators(LAs), they are often connected with the multi-stage looped TAHE to form a high-power multi-stage looped TAEG. The LAs can be connected in series with the previous and the subsequent segment in the

* Corresponding author.
** Corresponding author.
E-mail addresses: bitianjiao@qust.edu.cn (T. Bi), zhhwoo@mail.ipc.ac.cn (Z. Wu), liminzhang@mail.ipc.ac.cn (L. Zhang), jingyuan.xu@kit.edu (J. Xu), ecluo@mail.ipc.ac.cn (E. Luo), lichao201408@163.com (C. Li), cw_19344616@aliyun.com (B. Zhang), cw_19344616@aliyun.com (W. Chen).

Nomenclature

A	area, m^2
A_s	solid area, m^2
c_p:	isobaric heat capacity per unit mass, J/(kg·K)
f_κ	spatially averaged complex thermal function
f_ν	spatially averaged complex viscous function
H_2	total power, W
i	imaginary unit, $\sqrt{-1}$
k	thermal conductivity, W/(m·K)
k_s	thermal conductivity of solid, W/(m·K)
p_1	first-order oscillating pressure, Pa
$\|p1in\|$	Amplitudes of acoustic oscillation in the front cavity of LA, bar
p_m	mean pressure, Pa
Re	electric resistance, Ω
T_m	mean temperature, K
q	heat per unit length, W/m
U_1	oscillating volume velocity, m^3/s
W_a	Output acoustic power, kW
W_e	output electric power, kW
x	x coordinate, m
η_{ae}	acoustic-to-electric efficiency
η_{ta}	thermoacoustic efficiency
η_{te}	thermal-to-electric efficiency
σ	Prandtl number
ω	radian frequency, $2\pi f$, Hz
γ	ratio of isobaric specific heat to isochoric specific heats
ρ_m	mean density, kg/m^3
ε_s	correction factor for finite solid heat capacity
Re(Z)	real part of the acoustic impedance
Im(Z)	imaginary part of the acoustic impedance

multi-stage looped TAEG [13] or used as a side-branched load [7]. According to our experience, the side-branched connection mode of LAs is more suitable than the series connection mode for the high-power multi-stage looped TAEG because the side-branched connection mode has relatively low coupling strength with the multi-stage looped TAHE. Moreover, the large displacement of the pistons and strong vibration of LAs make the side-branched and dual-opposed configuration an appropriate mode, of which the strong vibration can be canceled out in some degree. Therefore, the combination of dual-opposed LAs and a multi-stage looped TAHE is a promising candidate for high-power TAEG.

Resonance tube(RT) is the most commonly used component connecting LAs and the multi-stage looped TAHE. It has a simple structure but a complex function. Changing the geometry or dimension of RT is an effective way to tune the acoustic field and improve the performance of a looped thermoacoustic system. With respect to geometry, Ali Al-Kayiem proposed a looped TAEG with a bypass pipe, the numerical simulation showed that it can achieve comparable performance as other types of travelling-wave TAEG [14]. Hamood found that introducing an inertance-compliance-inertance pipe into a two-stage looped TAEG to replace an original pipe with a constant diameter can reduce the pipe length but with the same levels of performance [15]. A Kruse numerically compared three methods of changing the geometry of the resonance tube, including inserting a side-branched stub, a compliant segment and an inertial segment, investigating the acoustic field adjustment by the three methods [16]. With respect to dimension, Xu and Hu [17] connected multiple engine stages and a cooler stage in a loop by RTs with different diameters, the simulation indicated that the area ratio between two adjacent RTs was a crucial factor in achieving efficient thermoacoustic conversion and power transmission. In the experiment, a multi-stage looped thermoacoustically-driven cryocooler with different diameter RTs was built and the advantage of this new structure was validated [18].

Given the literature reviewed above, the influence of geometry and diameter of RTs on looped thermoacoustic system have been thoroughly investigated, however, the influence of the length of RTs on multi-stage looped TAEG has not been reported before. In this paper, the influence of the length of RTs on multi-stage looped TAEG is numerically studied based on the decoupling-coupling idea which was proposed by Wang [19]. A multi-stage looped TAHE and LA 3-step coupling method is presented, which can be used to reveal the important function of the RTs in the coupling of the multi-stage looped TAHE and LAs. Experiments of the multi-stage looped TAEG with RTs of 1.5 m and 2 m are also conducted. The operating characteristics including the frequency, the oscillating pressure in the front cavity of LAs, the thermoacoustic conversion characteristic and the thermal-to-electric conversion characteristic are studied to demonstrate the influence of the length of RTs. In the rest of the paper, firstly, the system structure of the multi-stage looped TAEG is presented. Next, the multi-stage looped TAHE and LA 3-step coupling method is introduced thoroughly. Then the influence of the length of RTs on the multi-stage looped TAEG is analyzed based on the proposed coupling method and verified by experiments. Finally, some conclusions are given.

2. System structure

2.1. 4-Stage looped TAHE

Fig. 1 shows the schematic of the 4-stage looped TAHE which mainly consists of four identical TAHE units and four loads connected by four RTs. Each TAHE unit is primarily composed of a main ambient heat exchanger, a regenerator, a heater block, a thermal buffer tube, and a second ambient heat exchanger. The main ambient heat exchanger and second ambient heat exchanger are cooled by water at an ambient temperature of 25 °C. The heater block is heated by 36 heat cartridges which are tightly inserted in the holes at the rim of it. The heat cartridges

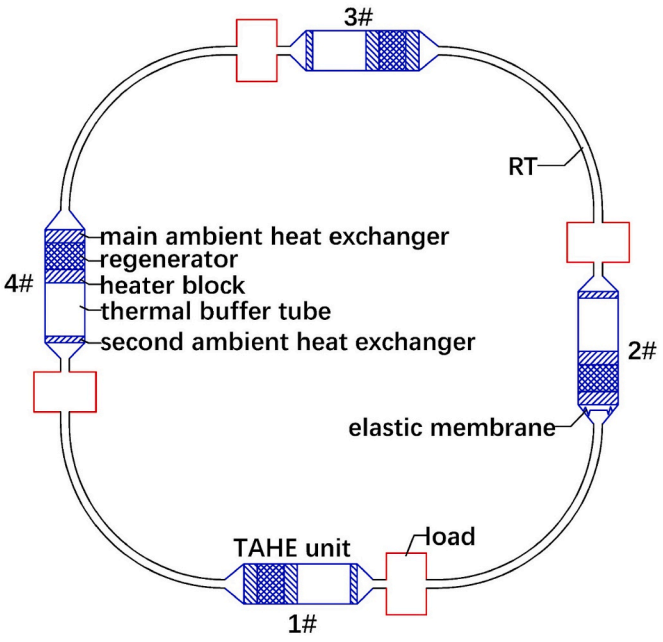

Fig. 1. Schematic of the 4-stage looped TAHE (TAHE: thermoacoustic heat engine, RT: resonance tube).

are specially designed as an "L" shape which can be installed conveniently as shown in Fig. 2. A maximum heating power of approximately 10 kW can be supplied to heat cartridges to maintain the heater block at the temperature of 650 °C. The regenerator is in essence a type of porous media that consists of stainless-steel wire mesh and provides a space for a thermoacoustic conversion. When the temperature of the heater block reaches the critical value of oscillation, the thermoacoustic effect can be induced spontaneously in the regenerator and the thermal energy can be converted to acoustic power. The thermal buffer tube and second ambient heat exchanger work as thermal insulators to prevent the load from the damage of high temperature arising from the heater block before it. The regenerator, heater block, and thermal buffer tube are coated with two blocks of Al_2O_3 insulation material of which the thickness is about 100 mm. A 2 mm thick elastic membrane is placed in the front of TAHE unit 2# to suppress the DC flow (or named Gedeon flow) [20] —a second-order time-averaged mass flow that is unwished but inevitable in a looped thermoacoustic network. Four RTs are used to connect the four TAHE units and loads to form the acoustic network. The detailed parameters of the TAHE unit are tabulated in Table 1.

At the output of each TAHE unit, a load is directly connected to it. The load can be viewed as the functional element of multi-stage looped TAHE. When the load is an acoustic-to-electric transducer such as LA or loudspeaker, the multi-stage looped TAHE can convert thermal energy to acoustic power and the acoustic-to-electric transducer can convert acoustic power to electric power in turn. This multi-stage thermoacoustic system is a multi-stage looped TAEG. When the load is a refrigerator such as a pulse tube refrigerator, the multi-stage looped TAHE can convert thermal energy to acoustic power and the pulse tube refrigerator can convert acoustic power to cold energy. This multi-stage thermoacoustic system is a multi-stage thermoacoustic refrigerator. From an acoustic point of view, either LA or pulse tube refrigerator can be viewed as an acoustic load of the TAHE unit and they have in essence the same function for the TAHE unit, i.e. consume the acoustic power produced by thermoacoustic effect.

2.2. Dual-opposed linear alternator

For high-power generation, subtly designed dual-opposed LA is selected as a load of TAHE unit. The photograph of dual-opposed LA is shown in Fig. 3(a). Two identical motors labeled 1# and 2# are placed oppositely and connected by the shell of the LA. In the front and back of the shell, two holes with appropriate diameters have been perforated to connect the LA with the TAHE unit and the RT, respectively. On the shell of motor 1# and motor 2#, the cooling water flows through the copper tubes to take away the waste heat produced by the LA. The connection

Table 1
Detailed parameters of TAHE unit.

Segment	Length/ mm	Diameter/ mm	Others
main ambient heat exchanger	60	80	Spacing of fins: 1 mm, porosity: 0.4.
regenerator	60	80	Filled with 120 mesh stainless-steel wire meshes, porosity: 0.8.
heater block	80	80	Spacing of fins: 1 mm, porosity: 0.48.
thermal buffer tube	125	80	\
second ambient heat exchanger	40	80	Spacing of fins: 1 mm, porosity: 0.48.
RT	2000/ 1500	20	\

form of the TAHE unit and dual-opposed LA is shown in Fig. 3(b). For the detailed parameters of the LA, please refer to Reference [12].

2.3. 4-Stage looped TAEG

After connecting 4-stage looped TAHE, LAs, and RTs, the 4-stage looped TAEG is built as shown in Fig. 4. There are mainly three circuits in the system. The first circuit is the cooling water circuit. The cooling water is produced by two sets of water chilling units (not shown in Fig. 4) and then pumped through the main ambient heat exchanger, second ambient heat exchanger, and the LA one by one, and finally returned to the water chilling units. The second circuit is the heating electric circuit. The electric wires from the power distribution cabinet are connected to the transformer, then the dynamometer, and finally the heat cartridges. The last circuit is the electric circuit of the LA, which connects the LA, load electric resistance, and electric capacitance. In the experiment, high purity (99.999 %) and pressurized helium gas with 6 MPa is used as the working substance. The heating temperature of the heater block is 650 °C and the temperature of the cooling water is 25 °C.

3. Coupling method

In the 4-stage looped TAEG, we decouple the system into two subsystems, namely the multi-stage looped TAHE and four dual-opposed LAs. In this section, firstly the modeling strategy of the output performance of multi-stage looped TAHE based on DeltaEC software is presented. The meaning of the output performance of multi-stage looped TAHE is that with different output acoustic impedance (the output oscillating pressure divided by the output oscillating volume velocity of the TAHE unit), the multi-stage looped TAHE has different operating

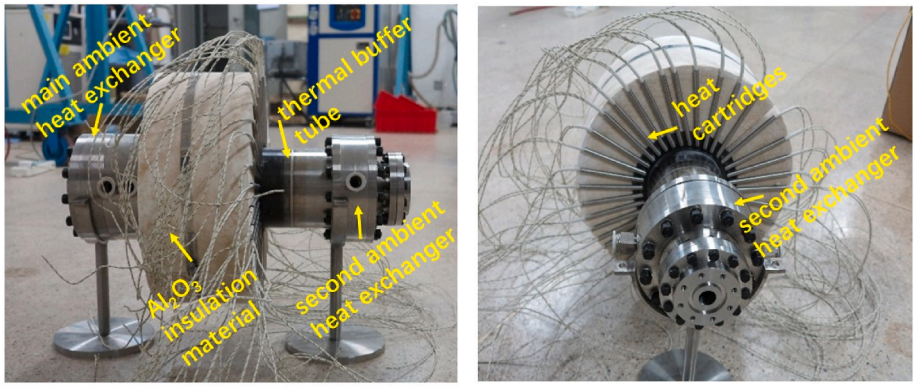

(a) (b)

Fig. 2. Photographs of the (a) front and (b) right views of the TAHE unit (regenerator and heater block are covered by the white Al_2O_3 insulation material, another block of Al_2O_3 insulation material which originally covers the thermal buffer tube is removed to show the "L" shape of heat cartridges, TAHE: thermoacoustic heat engine).

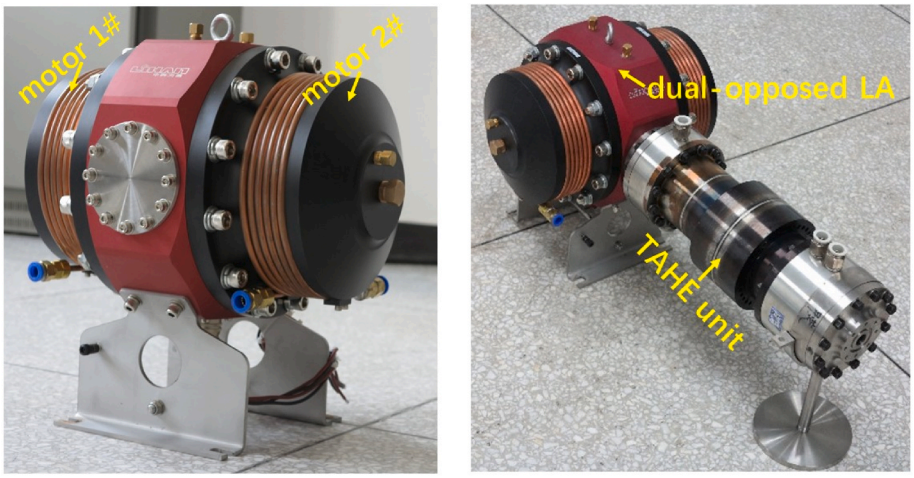

(a) (b)

Fig. 3. Photographs of the (a) dual-opposed LA (b) TAHE unit and dual-opposed LA (the heat cartridges and Al_2O_3 insulation material are not installed in the TAHE unit for clarity, TAHE: thermoacoustic heat engine, LA: linear alternator).

characteristics, such as output acoustic power and thermoacoustic efficiency. Secondly, an acoustic-mechanical-electrical coupling equivalent circuit model [12] to investigate the input performance of dual-opposed LA is briefly introduced. The meaning of the input performance of LA is that with different input acoustic impedance (the input acoustic oscillating pressure divided by the input oscillating volume velocity of the LA), the LA has different operating characteristics, such as acoustic-to-electric efficiency. Finally, a 3-step multi-stage looped TAHE and LA coupling method is proposed.

3.1. Modeling strategy of the output performance of multi-stage looped TAHE

The multi-stage looped TAHE is modeled based on DeltaEC software, which is one of the most commonly used simulation tools in the thermoacoustic research area. DeltaEC supplies users with a large number of segments including physical segments and logistical segments. The physical segments such as DUCT, CONE, HX (heat exchanger), and so on correspond to the real components of a thermoacoustic system and the users can connect the segments of DeltaEC in the same order with the experimental system. The logistical segments such as BEGIN, TBRANCH, and HARDEND can be viewed as virtual components, which are often used in the beginning, branch, and ending of the experimental system implying the structure of the acoustic network. After connecting the segments in the order of the experimental system, and defining appropriate boundary conditions, DeltaEC will integrate oscillating pressure, oscillating volume velocity et al. in the x direction (the axial direction of the system) depending on the following equations which have low-amplitude acoustic approximation and sinusoidal time dependence [21]:

$$dU_1 = \frac{i\omega A dx}{\gamma p_m}[1+(\gamma \quad 1)f_\kappa]p_1 + \frac{(f_\kappa \quad f_\upsilon)}{(1 \quad f_\upsilon)(1 \quad \sigma)}\frac{dT_m}{T_m}U_1 \tag{3.1}$$

$$dp_1 = \frac{i\omega\rho_m dx}{A(1 \quad f_\upsilon)}U_1 \tag{3.2}$$

$$H_2 = \frac{1}{2}\mathrm{Re}\left[p_1\widetilde{U}_1\left(1 \quad \frac{f_\kappa \quad \widetilde{f}_\nu}{(1+\varepsilon_s)(1+\sigma)(1 \quad \widetilde{f}_\nu)}\right)\right] + \frac{\rho_m c_p|U_1|^2}{2A\omega(1 \quad \sigma^2)|1 \quad f_\upsilon|^2}\mathrm{Im}\left[\widetilde{f}_\nu + \frac{(f_\kappa \quad \widetilde{f}_\nu)(1+\varepsilon_s f_\nu/f_\kappa)}{(1+\varepsilon_s)(1+\sigma)}\right] (Ak + A_s k_s)\frac{dT_m}{dx} \tag{3.3}$$

$$\frac{dH_2}{dx} = q \tag{3.4}$$

in which the meaning of the letters is listed in the Nomenclature. Eqn (3.1) is the thermoacoustic version of continuity equation. Eqn (3.2) is the thermoacoustic version of momentum equation. These two equations can be used to solve the dynamic variables: oscillating pressure p_1 and oscillating volume velocity U_1. Eqn (3.3) is the thermoacoustic version of energy conservation equation in the x direction. The variable H_2 is the total power in thermoacoustic system, which is the power carried in the x direction by the second-order thermoacoustic effect. Eqn (3.4) is the energy conservation equation in the lateral direction because the heat is input into TAHE in the lateral direction of heater block (i.e. perpendicular to the acoustic waveguide). After the integration is completed, the variables including the temperature, oscillating pressure, volume velocity, acoustic power, and total power along the x direction can be obtained. The output acoustic power and thermoacoustic efficiency of multi-stage looped TAHE can be calculated accordingly.

Fig. 5 shows the coupling model of multi-stage looped TAHE and LA. The multi-stage looped TAHE, BRANCH IMPEDANCE, and RT (shown in the red box) are modeled by DeltaEC software, while LA (shown in the green box) is modeled by MATLAB software which will be briefly introduced in the next subsection. In the modeling of the multi-stage looped TAHE and RT, because the stage number is four and the periodic symmetry of the acoustic network, the amplitude of the output variables of RT and input variables of the multi-stage looped TAHE is the same, while the phase difference is 90° (360° divided by four). A SOFTEND segment is used to realize the boundary conditions.

The LA is modeled in a separate MATLAB file. The coupling of multi-stage looped TAHE in DeltaEC software and LA in MATLAB software is accomplished by the use of the BRANCH IMPEDANCE segment. The BRANCH IMPEDANCE segment is a side branch with a specified impedance [21]. From an acoustic point of view, the nature of any load such as LA is an acoustic impedance. The LA can be viewed as an acoustic impedance represented by the BRANCH IMPEDANCE segment connected to the multi-stage looped TAHE. After the convergence of the program, the acoustic impedance of the BRANCH IMPEDANCE can be changed to investigate the output performance of the multi-stage looped TAHE. In the multi-stage looped TAHE model, the acoustic impedance of the BRANCH IMPEDANCE is the output acoustic impedance of multi-stage looped TAHE.

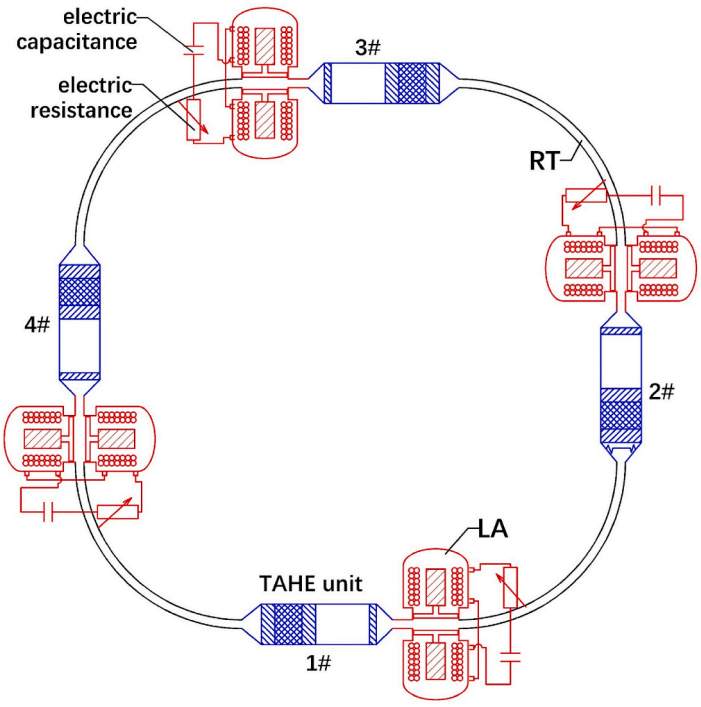

(a)

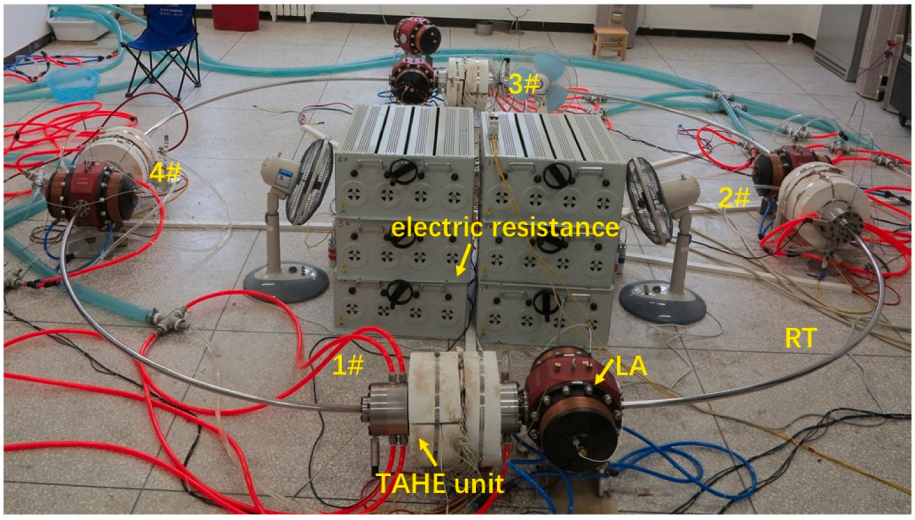

(b)

Fig. 4. (a) Schematic and (b) photograph of 4-stage looped TAEG (TAHE: thermoacoustic heat engine, LA: linear alternator, RT: resonance tube, TAEG: thermoacoustic electric generator).

3.2. Modeling strategy of the input performance of LA

The LA is a typical multi-physics coupling device. It couples the acoustic field, mechanical field, and electrical field. Because the input power is acoustic power (pressure oscillation) and the components with acoustic characteristics such as the back cavity are included in the LA, the acoustic field is one of the three coupling physics fields. The mechanical field manifests itself as the components with mechanical characteristics such as the mass of the piston, the suspension stiffness of the plate spring, and the mechanical resistance of the piston are included in the LA. The electric field must be considered since the output power of the LA is electric power and the electric components connected to the LA including electric resistance and electric compliance are important in the analysis. We have proposed an acoustic-mechanical-electrical coupling equivalent circuit model [12] of dual-opposed LA and this model will be used in the coupling between the multi-stage looped TAHE and LA. This model is introduced in the Appendix.

After establishing the LA model, and adjusting the parameters such as frequency, electric capacitance, electric resistance and mean pressure, the performance of LA such as acoustic-to-electric efficiency can be obtained. The acoustic impedance at the entrance of LA can be obtained according to the oscillating pressure and volume velocity in this position. If the frequency and electric resistance are changed, the acoustic impedance at the entrance and the performance of LA will change accordingly.

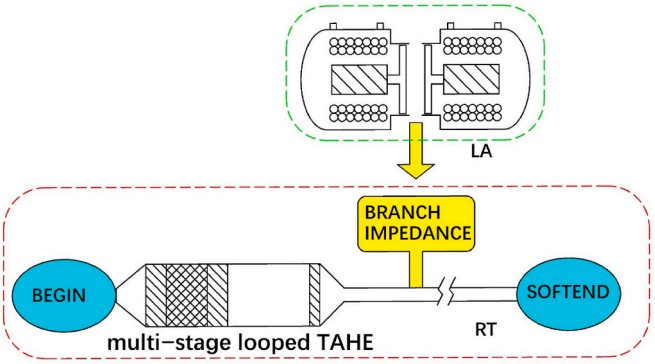

Fig. 5. Coupling of multi-stage looped TAHE and LA through the use of the BRANCH IMPEDANCE segment (TAHE: thermoacoustic heat engine, LA: linear alternator).

3.3. 3-Step multi-stage looped TAHE and LA coupling method

The coupling principles of the multi-stage looped TAHE and LA are as follows: 1. The oscillating frequency of the multi-stage looped TAHE and LA must be the same because the multi-stage looped TAHE and LA are connected as a system and they must share the same frequency. 2. The output acoustic impedance of multi-stage looped TAHE and the input acoustic impedance of LA must be the same because the export of multi-stage looped TAHE is the import of LA and the continuity of the acoustic parameters including the oscillating pressure and volume velocity. In this paper, the acoustic impedances are expressed in a real-imaginary part form. Therefore, the second principle can be divided into two principles: the real part (Re(Z)) and imaginary part (Im(Z)) of the output acoustic impedance of multi-stage looped TAHE must be the same as the Re(Z) and Im(Z) of the input acoustic impedance of LA, respectively. Hence, the coupling principles can be summarized as follows: 1. The equivalent frequency. 2. The equivalent Re(Z). 3. The equivalent Im(Z).

The coupling method of multi-stage looped TAHE and LA is shown in Fig. 6 -Fig. 8. It includes three steps. Step 1: Calculate the output performance of multi-stage looped TAHE, which is shown in Fig. 6. Step 2: Calculate the input performance of LA, which is shown in Fig. 7. Step 3: Couple the output performance of multi-stage looped TAHE and the input performance of LA, which is shown in Fig. 8. The three steps will be introduced in detail in the rest of the subsection.

Step 1: Calculate the output performance of multi-stage looped TAHE. To obtain the output performance of multi-stage looped TAHE under different output acoustic impedances, two independent acoustic impedance ranges are assigned to Re(Z) and Im(Z) of the BRANCH IMPEDANCE segment (graph 1 of Fig. 6).

The DeltaEC software will increase the Re(Z) and Im(Z) of the BRANCH IMPEDANCE segment linearly and independently by many safe and small enough steps from the lower limits to the upper limits. Because the increments of Re(Z) and Im(Z) are independent, the acoustic impedance will form a matrix in which the row is Im(Z) from the lower limit to the upper limit and the column is Re(Z) from the lower limit to the upper limit. Each element in the acoustic impedance matrix contains one Re(Z) and one Im(Z), and it will be input into the multi-stage looped TAHE model. After running the DeltaEC program, one frequency with other important working characteristics will be obtained. According to the coupling principles mentioned in the last paragraph, only the frequency and acoustic impedance are concerned in the coupling progress. Hence, Re(Z)-Im(Z)-frequency 3D surface plot can be obtained (graph 3 of Fig. 6).

Step 2: Calculate the input performance of LA. The LA is the acoustic load of multi-stage looped TAHE, and the different lengths of the RTs will influence the frequency and then the input performance of LA. Hence, frequency is one variable that should be considered in the input

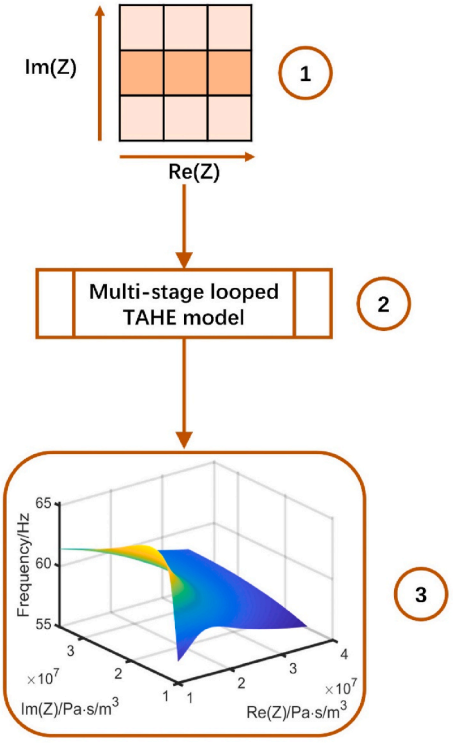

Fig. 6. Step 1 of multi-stage looped TAHE and LA coupling method (TAHE: thermoacoustic heat engine, LA: linear alternator, Re(Z): real part of output acoustic impedance, Im(Z): imaginary part of output acoustic impedance).

performance of LA. Another variable that should be considered is the electric resistance (Re) connected to the LA which can strongly influence the input performance of LA and can be easily changed in the experiment by the use of rheostat. Therefore, the frequency and electric resistance are two variables that will be linearly changed (graph 4 of Fig. 7). After changing electric resistance and frequency linearly and independently, these two variables will form a matrix in which the row is the frequency from the lower limit to the upper limit and the column is electric resistance from the lower limit to the upper limit (graph 4 of Fig. 7). Each element in the variable matrix contains one electric resistance and one frequency, and it will be input to the LA model, one Re(Z) and one Im(Z) of the input acoustic impedance with other important working characteristics will be obtained. Therefore, Re-frequency-Re(Z) and Re-frequency-Im(Z)) 3D surface plots can be drawn (graphs 6 and 7 of Fig. 7). We can cut the 3D surface plots in graph 6 and graph 7 using the Re = 60 Ω plane, and obtain the 2D frequency-Re(Z) plot and frequency-Im(Z) plot (graphs 8 and 9 of Fig. 7). In these two graphs, the frequency has a one-to-one corresponding relationship with Re(Z) and Im(Z). Therefore, under electric resistance of 60 Ω, the Re(Z)-Im(Z)-frequency 3D line plot can be obtained (graph 10 of Fig. 7).

Step 3: Couple the output performance of multi-stage looped TAHE and the input performance of LA. After obtaining the output performance 3D surface of multi-stage looped TAHE as shown in graph 3 of Fig. 6 and the input performance 3D line of LA as shown in graph 10 of Fig. 7, we can plot the surface and line in one Re(Z)-Im(Z)-frequency coordinate (graph 11 of Fig. 8).

The intersection point (yellow point in graph 11 of Fig. 8) is the coupling point, and this point satisfies 3 coupling principles: 1. The equivalent frequency 2. The equivalent Re(Z) 3. The equivalent Im(Z). Hence, the coupling point is the working point of multi-stage looped TAEG when the LA is connected with an electric resistance of 60 Ω. The frequency corresponding to the working point is the oscillating frequency of multi-stage looped TAEG and the Re(Z) and Im(Z) form the output acoustic impedance of multi-stage looped TAHE as well as the

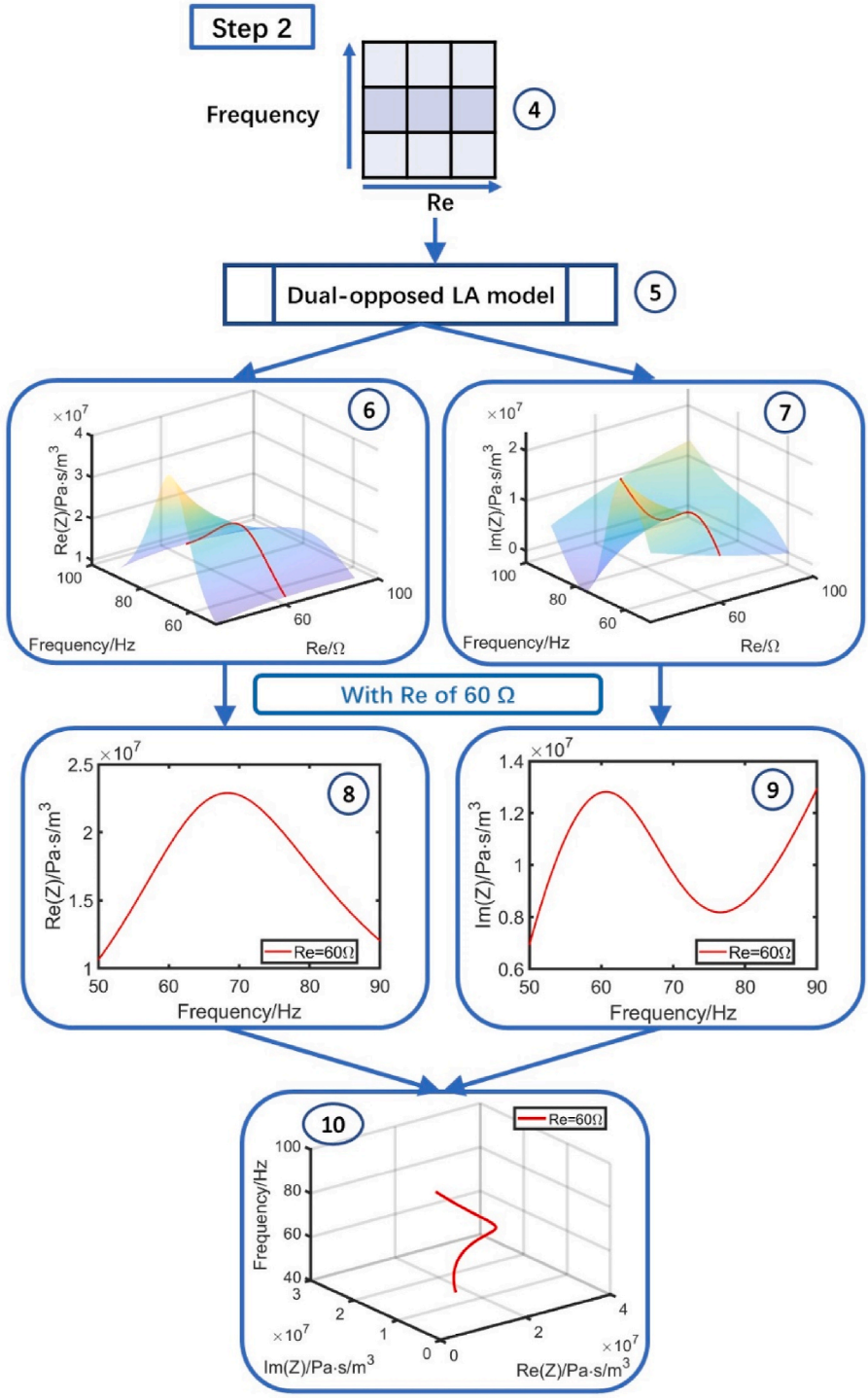

Fig. 7. Step 2 of multi-stage looped TAHE and LA coupling method (TAHE: thermoacoustic heat engine, LA: linear alternator, Re: electric resistance, Re(Z): real part of input acoustic impedance, Im(Z): imaginary part of input acoustic impedance).

input acoustic impedance of LA. After obtaining the oscillating frequency and acoustic impedance, the other working characteristics of multi-stage looped TAHE and LA can be acquired by the multi-stage looped TAHE model and LA model.

4. Numerical study and experimental validation

In this paper, two sets of RTs with lengths of 1.5 m and 2 m are installed in the 4-stage looped TAEG to investigate the influence of length of RTs on multi-stage looped TAEG.

4.1. The output performance of multi-stage looped TAHE with different RTs

After establishing the DeltaEC models of multi-stage looped TAHE with 1.5 m RTs and 2 m RTs, two acoustic impedance matrices should be assigned to the BRANCH IMPEDANCE segments according to step 1 of the coupling method in section 3.3. The appropriate acoustic impedance matrices for the BRANCH IMPEDANCE segments with different RTs are different according to the convergence condition of the models and our experiment experience. As shown in Fig. 9, an acoustic impedance range

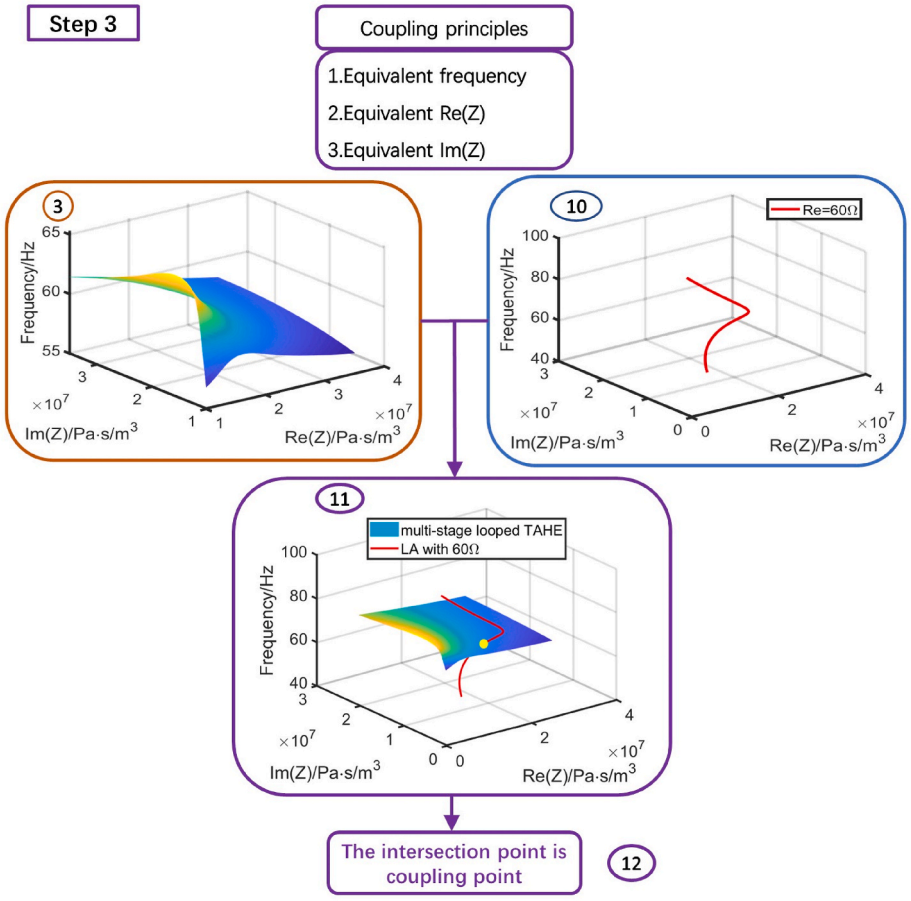

Fig. 8. Step 3 of multi-stage looped TAHE and LA coupling method (TAHE: thermoacoustic heat engine, LA: linear alternator, Re: electric resistance, Re(Z): real part of acoustic impedance, Im(Z): imaginary part of acoustic impedance).

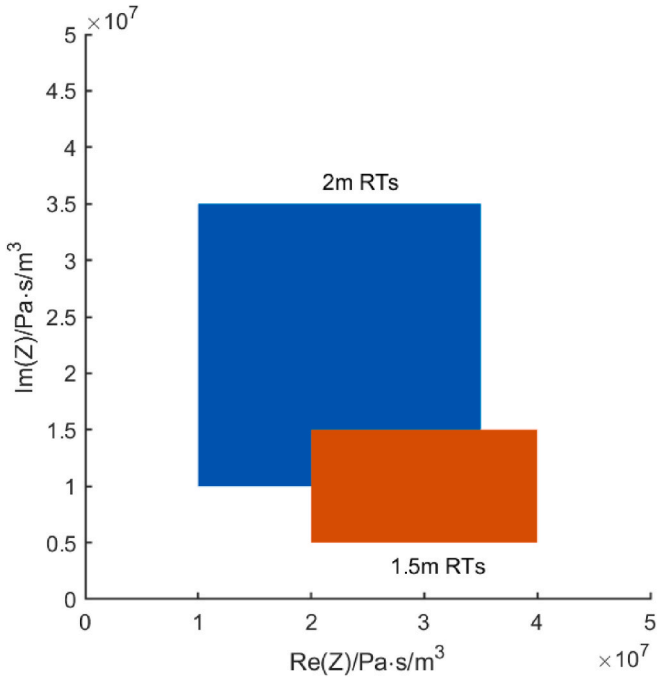

Fig. 9. Two different acoustic impedance matrices for the multi-stage looped TAHE model with 1.5 m RTs and 2 m RTs (Re(Z): real part of output acoustic impedance, Im(Z): imaginary part of output acoustic impedance, TAHE: thermoacoustic heat engine, RT: resonance tube).

of which the Re(Z) and Im(Z) all vary from 1×10^7 Pa s/m^3 to 3.5×10^7 Pa s/m^3 is selected for multi-stage looped TAHE with 2 m RTs while an acoustic impedance range of which the Re(Z) varies from 2×10^7 Pa s/m^3 to 4×10^7 Pa s/m^3 and the Im(Z) varies from 0.5×10^7 Pa s/m^3 to 1.5×10^7 Pa s/m^3 is selected for multi-stage looped TAHE model with 1.5 m RTs. From Fig. 9, we know that the 2 m RT multi-stage looped TAHE model has a relatively larger working acoustic impedance range than that of 1.5 m RT.

After inputting respective acoustic impedance matrices into the multi-stage looped TAHE DeltaEC model with 1.5 m RTs and 2 m RTs, operating characteristics can be acquired. Fig. 10 shows frequencies of the multi-stage looped TAHE with 1.5 m RTs and 2 m RTs. The frequency is an operating characteristic that influences the output performance of multi-stage looped TAHE and the input performance of LA simultaneously. The multi-stage looped TAHE and LA of one multi-stage looped TAEG share the same frequency when operating. Therefore, the choice of frequency is important to the coupling of multi-stage looped TAHE and LA. According to Fig. 10, with RTs of 2 m, the frequency of multi-stage looped TAHE varies from 60.2 Hz to 70 Hz while with RTs of 1.5 m, the frequency of multi-stage looped TAHE varies from 70.9 Hz to 76.4 Hz. The multi-stage looped TAHE can work at a higher frequency with RTs of 1.5 m. This conclusion agrees well with our experiment experience and can be explained qualitatively: due to almost the same structure of multi-stage looped TAHE with 1.5 m RTs and 2 m RTs, the acoustic wave structures are almost the same except the wavelength in multi-stage looped TAHE with 1.5 m RTs is shorter than that in multi-stage looped TAHE with 2 m RTs. The same working conditions including the working substance and temperature guarantee the same acoustic speed. According to the relationship of frequency(f), acoustic

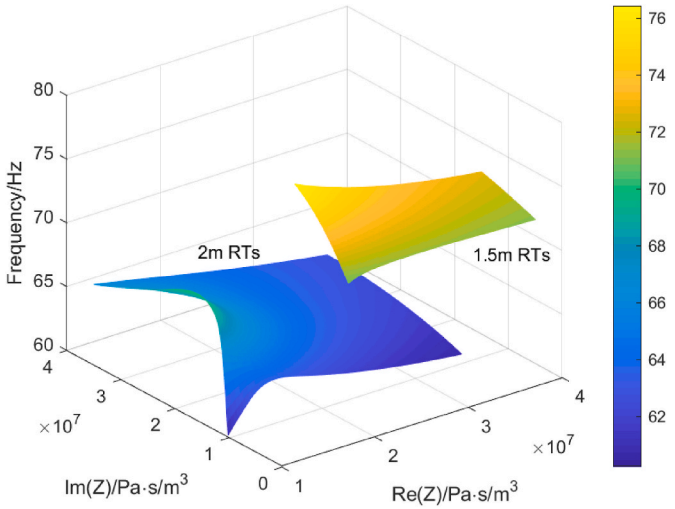

Fig. 10. Frequencies of the multi-stage looped TAHE with 1.5 m RTs and 2 m RTs (Re(Z): real part of output acoustic impedance, Im(Z): imaginary part of output acoustic impedance, TAHE: thermoacoustic heat engine, RT: resonance tube).

wave speed(a), and acoustic wavelength(λ): f = a/λ, the frequency of multi-stage looped TAHE with 1.5 m RTs is higher than that of multi-stage looped TAHE with 2 m RTs. Therefore, an appropriate choice of length of RTs can significantly determine the frequency of multi-stage looped TAHE and then the coupling between the multi-stage looped TAHE and LA.

Fig. 11 shows the output acoustic power of multi-stage looped TAHE with 1.5 m RTs and 2 m RTs. For multi-stage looped TAHE with 2 m RT, the low Re(Z) and Im(Z) result in low output acoustic power. When the Im(Z) is from 2.5 × 10^7 Pa s/m^3 to 3.5 × 10^7 Pa s/m^3, the output acoustic power can be relatively stable and high. The highest output acoustic power of 5.2 kW can be obtained in this range. For multi-stage looped TAHE with 1.5 m RT, the low Re(Z) and Im(Z) also result in low output acoustic power. When the Re(Z) and Im(Z) increase, the output acoustic power also increases. The highest output acoustic power of 3.9 kW can be obtained when the Re(Z) is 4 × 10^7 Pa s/m^3 and Im(Z) is 1.5 × 10^7 Pa s/m^3, which are all the upper limits of the acoustic impedance ranges for multi-stage looped TAHE with 1.5 m RT.

Fig. 12 shows the thermoacoustic efficiencies of multi-stage looped TAHE with 1.5 m RTs and 2 m RTs. For multi-stage looped TAHE with 2 m RT, there are two acoustic impedance points with extremely low thermoacoustic efficiency, i.e., Re(Z) = 1 × 10^7 Pa s/m^3, Im(Z) = 1 × 10^7 Pa s/m^3 and Re(Z) = 1 × 10^7 Pa s/m^3, Im(Z) = 4 × 10^7 Pa s/m^3. Considering the low output acoustic power when Re(Z) is 1 × 10^7 Pa s/m^3 and Im(Z) is 1 × 10^7 Pa s/m^3 as shown in Fig. 11, this point is a bad working acoustic impedance that should be avoided in the coupling with LA. When the Re(Z) is 1.3 × 10^7 Pa s/m^3 and Im(Z) is 1.27 × 10^7 Pa s/m^3, the thermoacoustic efficiency can achieve the highest value of 0.39 with 2 m RT. For multi-stage looped TAHE with 1.5 m RT, due to the relatively small acoustic impedance working range in Fig. 9, the thermoacoustic efficiency stabilizes at a relatively high level, varying from 0.25 to 0.37. When the Re(Z) is 2 × 10^7 Pa s/m^3 and Im(Z) is 0.91 × 10^7 Pa s/m^3, the thermoacoustic efficiency can achieve the highest value of 0.37 with 1.5 m RT, a little less than that of multi-stage looped TAHE with 2 m RT.

4.2. *Input performance of LA*

Fig. 13 shows the Re(Z) of LA with continuous frequency variation and electric resistance variation. In the experiment, the electric resistance is set at a series of discrete values, so the lines with some discrete electric resistances are also indicated in Fig. 13 and projected to a frequency-Re(Z) 2-D plane in Fig. 14. From these two figures, we can see that either the frequency or electric resistance can dramatically influence the Re(Z). With a fixed electric resistance, the Re(Z) firstly increases and then decreases with the increase of frequency. With all the electric resistances, the Re(Z) can get the maximum at the same frequency, i.e., 68.3 Hz. With a fixed frequency, the Re(Z) decreases with the increase of electric resistance.

Figs. 15 and 16 show the Im(Z) of LA with the variation of frequency and electric resistance. According to these two figures, we can see that either the frequency or the electric resistance can dramatically influence the Im(Z). With electric resistances of 40 Ω, 50 Ω, 60 Ω, and 70 Ω, the Im (Z) firstly increases, then decreases, and finally increases with the increase of frequency, a little bit like graphs of the sine function. The five lines with different electric resistances intersect at one point, i.e., 68.3 Hz and 1.1 × 10^7 Pa s/m^3. At a frequency beyond 68.3 Hz, the Im(Z) increases with the increase of electric resistance while at a frequency below 68.3 Hz, the Im(Z) decreases with the increase of electric

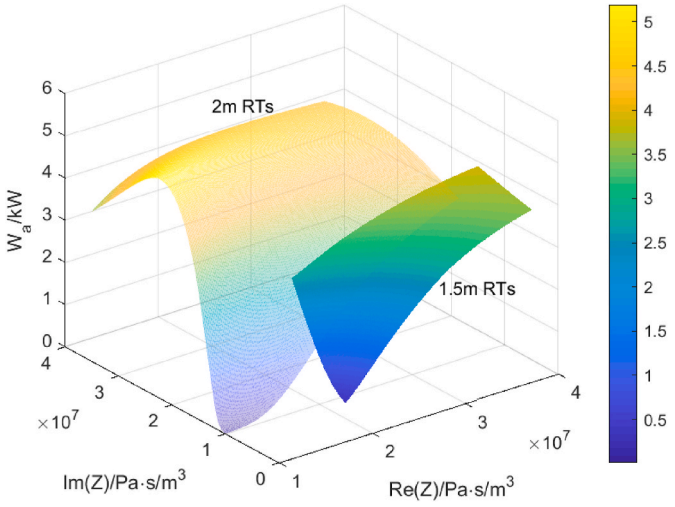

Fig. 11. Output acoustic power (W_a) of the multi-stage looped TAHE with 1.5 m RTs and 2 m RTs (The semitransparent surface is 2 m RTs while the opaque surface is 1.5 m RTs, Re(Z): real part of output acoustic impedance, Im(Z): imaginary part of output acoustic impedance, TAHE: thermoacoustic heat engine, RT: resonance tube).

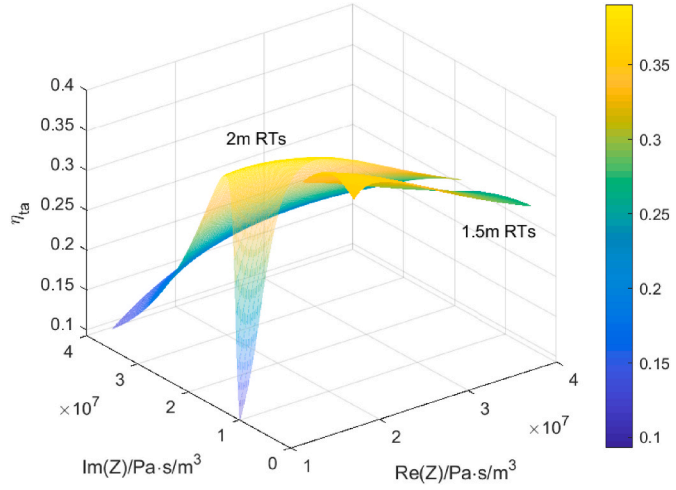

Fig. 12. Thermoacoustic efficiencies (η_{ta}) of the multi-stage looped TAHE with 1.5 m RTs and 2 m RTs (The semitransparent surface is 2 m RTs while the opaque surface is 1.5 m RTs, Re(Z): real part of output acoustic impedance, Im (Z): imaginary part of output acoustic impedance, TAHE: thermoacoustic heat engine, RT: resonance tube).

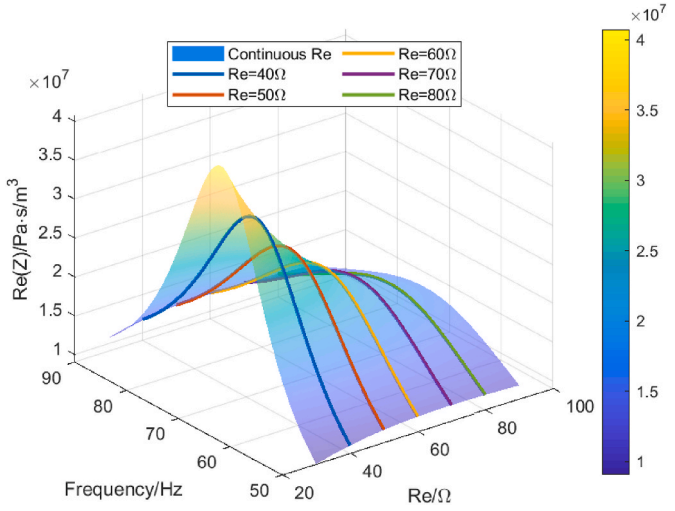

Fig. 13. The Real part of the input acoustic impedance (Re(Z)) of the linear alternator with continuous frequency variation and load electric resistance(Re) variation, Re(Z) with some discrete electric resistances are also indicated using lines with different colors. (For interpretation of the references to color in this figure legend, the reader is referred to the Web version of this article.)

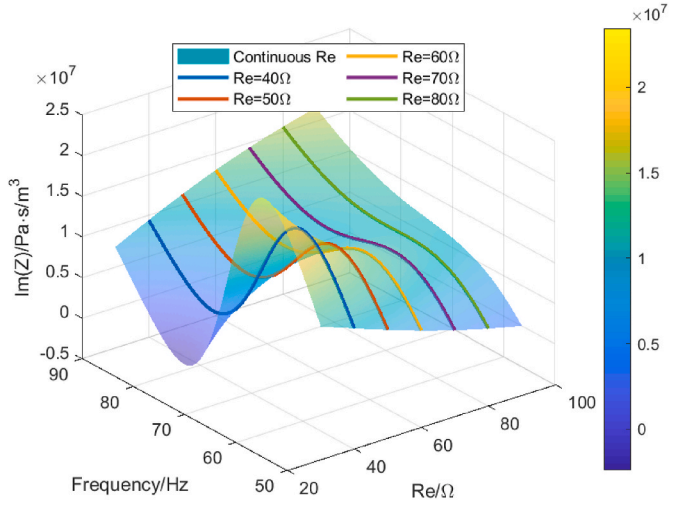

Fig. 15. Imaginary part of the input acoustic impedance (Im(Z)) of the linear alternator with continuous frequency variation and load electric resistance (Re) variation, Im(Z) with some discrete electric resistances are also indicated using lines with different colors. (For interpretation of the references to color in this figure legend, the reader is referred to the Web version of this article.)

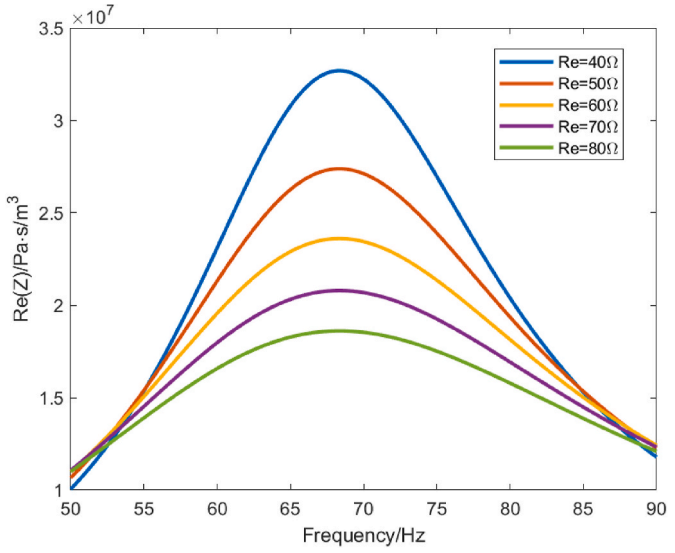

Fig. 14. Real part of the input acoustic impedance (Re(Z)) of the linear alternator with continuous frequency variation and discrete load electric resistance (Re) variation.

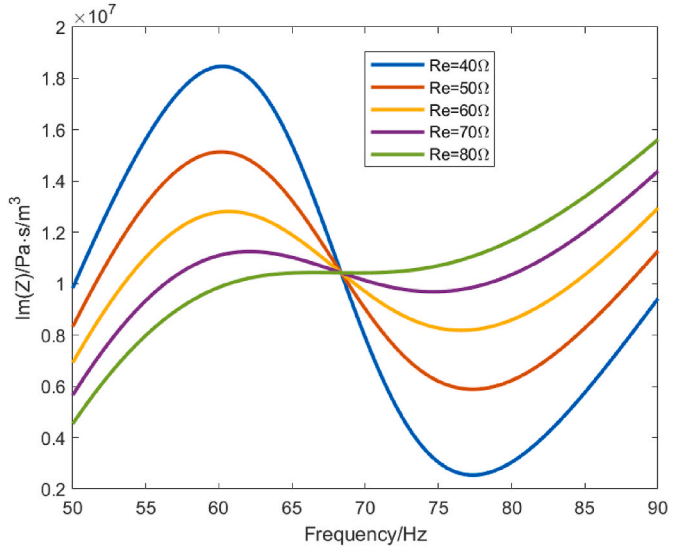

Fig. 16. Imaginary part of the input acoustic impedance (Im(Z)) of the linear alternator with continuous frequency variation and discrete load electric resistance (Re) variation.

resistance.

Figs. 17 and 18 show the acoustic-to-electric efficiency of LA with the variation of frequency and electric resistance. According to these two figures, we can see that either the frequency or the electric resistance can influence the acoustic-to-electric efficiency, but the influence is limited. The acoustic-to-electric efficiency can be maintained at a level higher than 0.65 despite the dramatic change in electric resistance and frequency. The relatively high and stable acoustic-to-electric efficiency of LA makes it a potential candidate for the acoustic-to-electric transducer of high-power multi-stage looped TAEG.

According to the coupling principles mentioned in section 3.3, Re(Z), Im(Z), and frequency are three variables that should be considered in the coupling progress. For the multi-stage looped TAHE, Fig. 10 is an appropriate figure used for coupling because its three axes are just Re (Z), Im(Z), and frequency. For the LA, the figure with three axes of Re(Z), Im(Z), and frequency for coupling can be obtained after some transformation of Figs. 14 and 16. According to these two figures, with a certain electric resistance, every frequency corresponding to one Re(Z) and one Im(Z). The one-to-one corresponding relationship with a certain electric resistance indicates that the relationship of the three variables namely Re(Z), Im(Z), and frequency can be drawn as a line in Re(Z)-Im (Z)-frequency 3-D coordinate. Different electric resistances make the lines different. After the transformation, the Re(Z)-Im(Z)-frequency 3-D plots of LA input performance are shown in Fig. 19.

4.3. *Coupling of multi-stage looped TAHE and LA*

The coupling of multi-stage looped TAHE and LA can be conducted in Re(Z)-Im(Z)-frequency coordinate shown in Fig. 20. The two surfaces labeled “2 m RTs” and “1.5 m RTs” are the frequencies of multi-stage looped TAHE under different output acoustic impedances with 2 m RTs and 1.5 m RTs, respectively, which are identical with Fig. 10. The

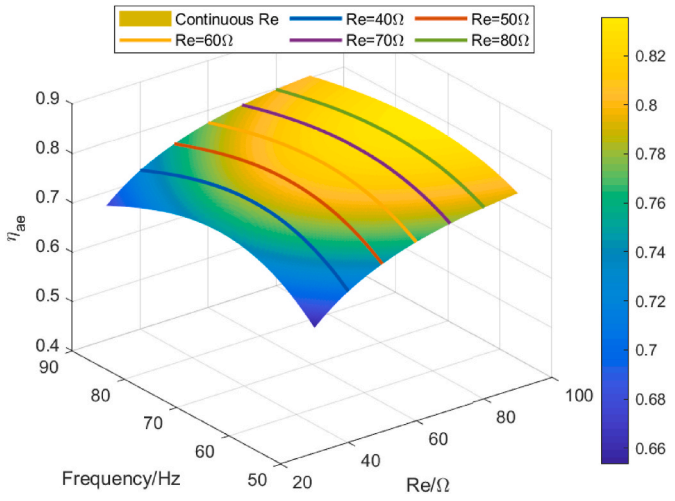

Fig. 17. Acoustic-to-electric efficiency(η_{ae}) of the linear alternator with continuous frequency variation and load electric resistance (Re) variation, acoustic-to-electric efficiency with some discrete are also indicated using lines with different colors. (For interpretation of the references to color in this figure legend, the reader is referred to the Web version of this article.)

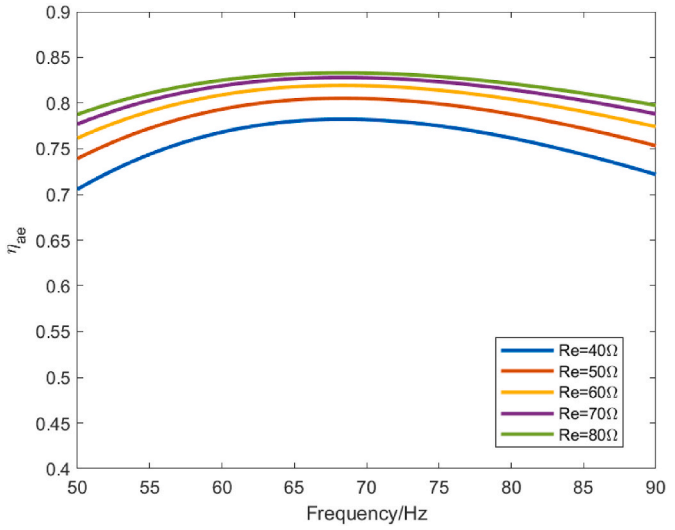

Fig. 18. Acoustic-to-electric efficiency(η_{ae}) of the linear alternator with continuous frequency variation and discrete load electric resistance (Re) variation.

colorful lines are the Re(Z)-Im(Z)-frequency 3-D lines which are the same with Fig. 19. The intersection points of multi-stage looped TAHE output performance surfaces and LA input performance lines are the working points of multi-stage looped TAEG with RTs of 1.5 m and 2 m. After obtaining the coordinates of the intersection points, i.e. the acoustic impedance (including Re(Z) and Im(Z)) and frequency, the output acoustic power and thermoacoustic efficiency of multi-stage looped TAHE can be acquired from Figs. 11 and 12, and the acoustic-to-electric efficiency of LA can be acquired from Fig. 17. Thus, the multi-stage looped TAEG performance can be obtained combining the performance of multi-stage looped TAHE and LA. Until now, the 3-step coupling method mentioned in section 3.3 has been accomplished. In the rest of this subsection, we will analyze the working characteristics of multi-stage looped TAEG with different length of RTs based on the results of the 3-step coupling method and experimental validation.

Fig. 21 shows Re(Z) and Im(Z) of output acoustic impedances of multi-stage looped TAHE (or input acoustic impedances of LA) with RTs

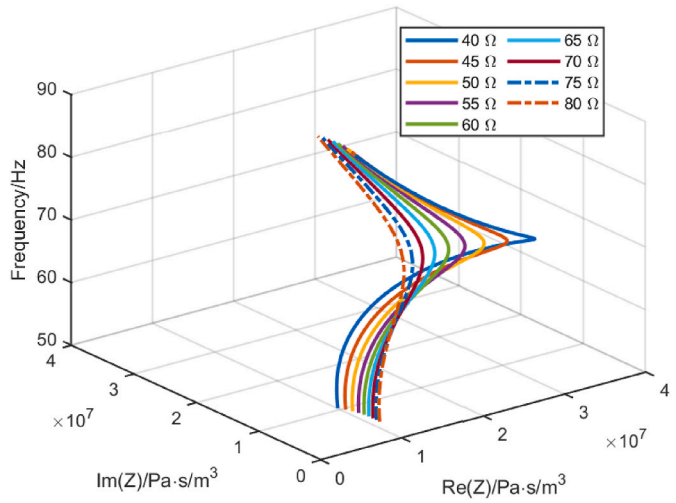

Fig. 19. Real part of the input acoustic impedance (Re(Z))-imaginary part of the input acoustic impedance (Im(Z))-frequency 3-D plots of the linear alternator, lines with different colors represent different load electric resistances (Re). (For interpretation of the references to color in this figure legend, the reader is referred to the Web version of this article.)

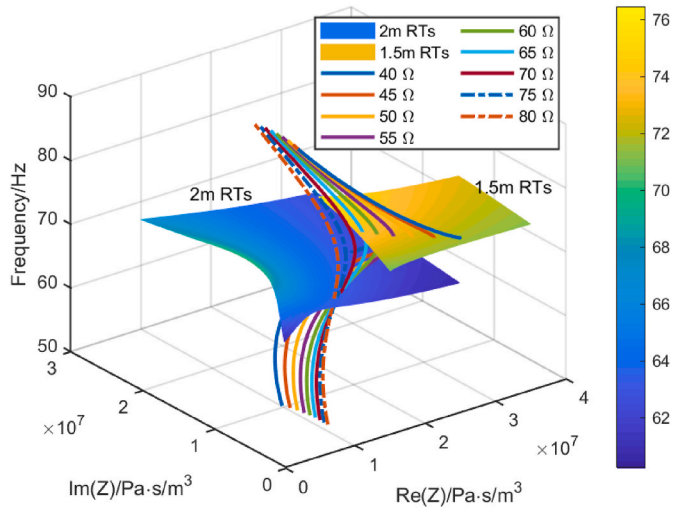

Fig. 20. Coupling of multi-stage looped TAHE and LA (the two surfaces labeled "2 m RTs" and "1.5 m RTs" are the frequencies of multi-stage looped TAHE under different output acoustic impedances with 2 m RTs and 1.5 m RTs, the colorful lines are the Re(Z)-Im(Z)-frequency 3-D lines of LA, Re(Z): real part of acoustic impedance, Im(Z): imaginary part of acoustic impedance).

of 1.5 m and 2 m under different electric resistances. From Fig. 20 we can see that all the lines with electric resistances from 40 Ω to 80 Ω can intersect with the 2 m RTs surface. Thus, the simulation results of multi-stage looped TAEG with 2 m RTs have 9 points as shown in Fig. 21. While the lines with electric resistances from 40 Ω to 65 Ω can intersect with 1.5 m RTs, so the simulation results of multi-stage looped TAEG with 1.5 m RTs have 6 points. Therefore, the multi-stage looped TAEG with 2 m RTs can work in a larger range of electric resistance than that with 1.5 m RTs. We can also find Re(Z) with RTs of 1.5 m and 2 m all decrease with the increase of electric resistance, but Im(Z) with RTs of 1.5 m and 2 m has a reverse trend.

Fig. 22 shows the frequencies of multi-stage looped TAEG with RTs of 1.5 m and 2 m under different electric resistances. According to Fig. 22, the frequencies in the experiment with RTs of 1.5 m are 70 Hz, 70.3 Hz, 70.8 Hz, 71.4 Hz and 72.4 Hz with the electric resistance increasing from 40 Ω to 60 Ω, and the frequencies in experiment with RTs of 2 m are

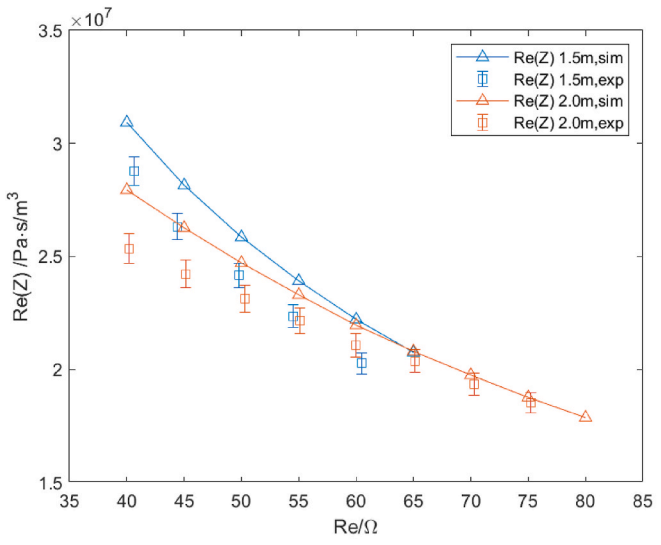

(a)

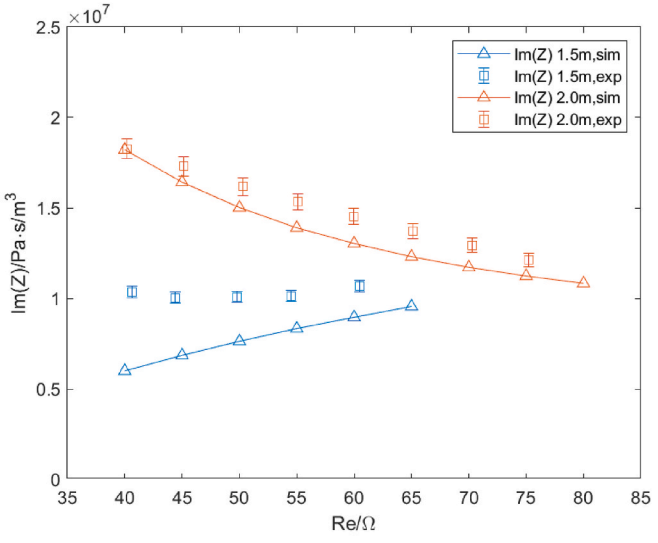

(b)

Fig. 21. (a) Real part of the acoustic impedance (Re(Z)) and (b) imaginary part of the acoustic impedance (Im(Z)) of multi-stage looped TAHE (or LA) with RTs of 1.5 m and 2 m under different load electric resistances (Re) (sim: simulation, exp: experiment, TAHE: thermoacoustic heat engine, LA: linear alternator).

63.6 Hz, 63.4 Hz, 63.1 Hz, 63 Hz, 62.9 Hz, 63.1 Hz, 63.3 Hz and 63.3 Hz with the electric resistance increasing from 40 Ω to 70 Ω. The frequency stabilizes at about 71 Hz and 63 Hz with RTs of 1.5 m and 2 m, respectively. For multi-stage looped TAEG, the length of RTs has a significant influence on the frequency, while the electric resistance connecting with LA has limited influence. Prolonging the length of RTs can decrease the frequency of multi-stage looped TAEG.

Fig. 23 shows amplitudes of acoustic oscillation in the front cavity of LA with RTs of 1.5 m and 2 m under different electric resistances. Based on our experimental experience, amplitudes of acoustic oscillation in the front cavity are an important variable that indicates the operating stability of multi-stage looped TAEG. When this variable is less than 2.5 bar, the multi-stage looped TAEG could probably evolve in unstable states—such as damping or frequency jumping. The damping will make the multi-stage looped TAEG stop working. The frequency jumping sometimes makes the displacements of pistons of LA exceed the maximum allowable displacement and causes great damage to the LA, which should be avoided in the experiment. Therefore, 2.5 bar is a

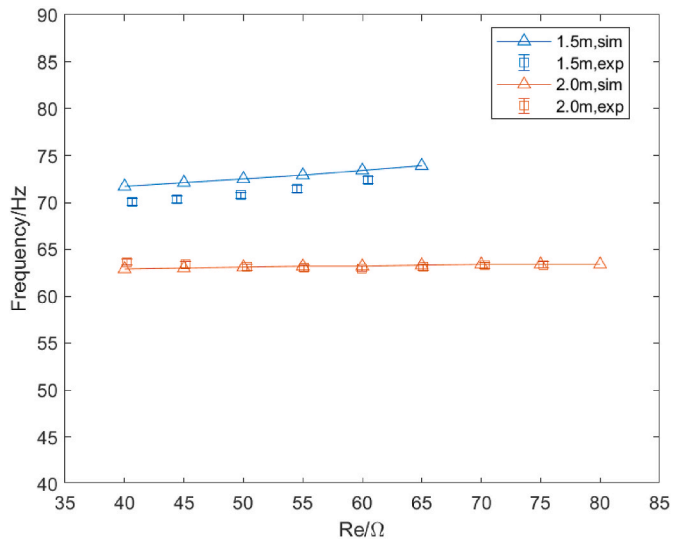

Fig. 22. Frequencies of multi-stage looped TAEG with RTs of 1.5 m and 2 m under different load electric resistances (Re) (sim: simulation, exp: experiment, TAEG: thermoacoustic electric generator, RT: resonance tube).

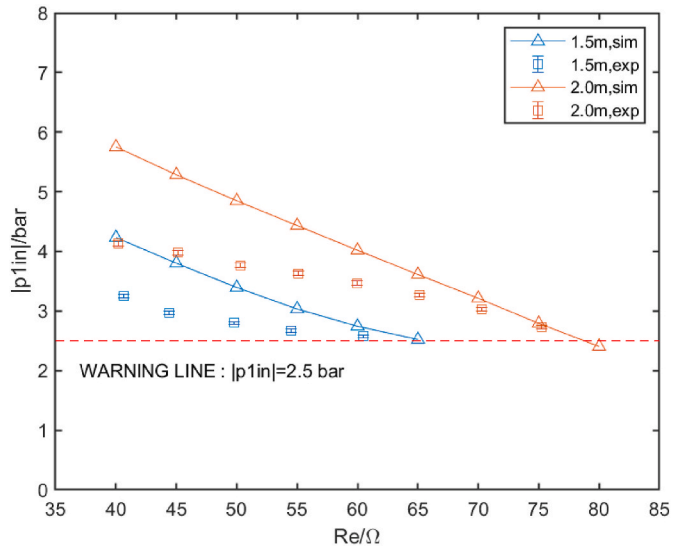

Fig. 23. Amplitudes of acoustic oscillation in the front cavity of LA (|p1in|) with RTs of 1.5 m and 2 m under different load electric resistances (Re) (The warning line is a stopping criterion when we increase electric resistance from 40 Ω, sim: simulation, exp: experiment, LA: linear alternator).

stopping criterion when we increase electric resistance from 40 Ω. Fig. 23 also shows that prolonging the length of RTs will increase the amplitude of acoustic oscillation in the front cavity. The maximum amplitude of acoustic oscillation in the experiment increases from 3.2 bar to 4.1 bar after the RTs are prolonged from 1.5 m to 2 m. At the same electric resistance, the amplitude of acoustic oscillation with 2 m RT is about 1 bar larger than that with 1.5 m RT in the experiment.

Fig. 24 shows the thermoacoustic conversion characteristics of multi-stage looped TAEG. From Fig. 24(a), we can find that increasing the electric resistance will decrease the output acoustic power with 1.5 m or 2 m RT. With the same electric resistance, prolonging the length of RTs can increase the output acoustic power of multi-stage looped TAEG. With the increase of the length of RTs from 1.5 m to 2 m, the maximum output acoustic power in the experiment increases from 6.97 kW to 8.16 kW. The output acoustic power in the simulation is larger than that in the experiment, and the difference increases with the decrease of electric

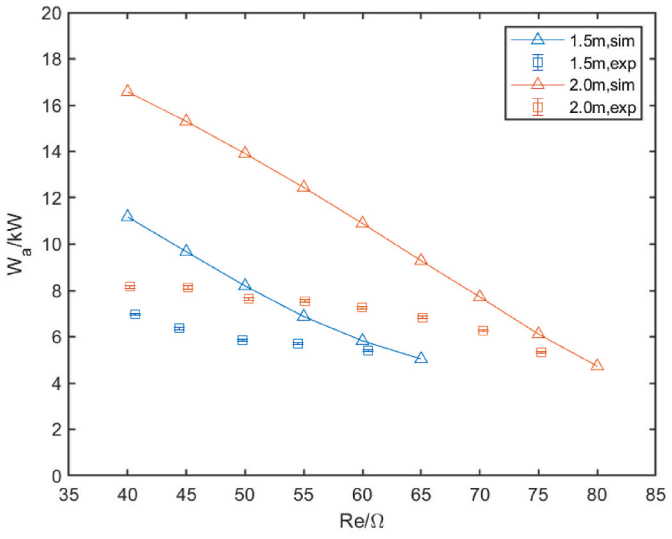

(a)

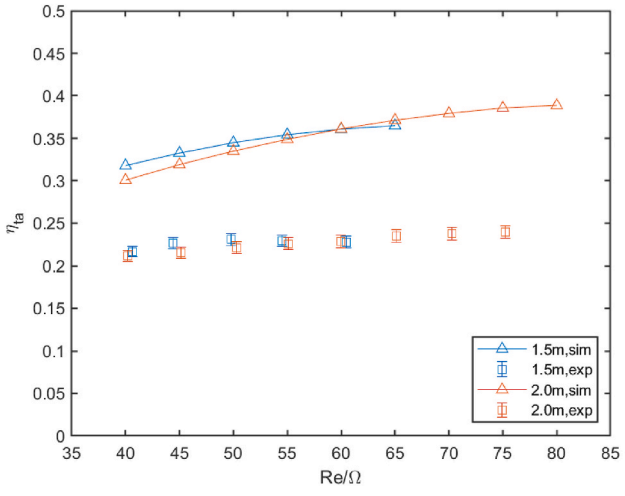

(b)

Fig. 24. (a) Output acoustic power (W_a) and (b) thermoacoustic efficiency (η_{ta}) of multi-stage looped TAEG with RTs of 1.5 m and 2 m under different load electric resistances (Re) (sim: simulation, exp: experiment, TAEG: thermoacoustic electric generator, RT: resonance tube).

resistance or increase of amplitudes of acoustic oscillation in the front cavity. The reason is that the acoustic power loss has been underestimated in the simulation. For example, RTs are assumed to be straight in simulation. However, they have 90-degree bends in the experiment to form a loop. Thus, the acoustic power loss due to the 90-degree bends is missing in the simulation. Some other acoustic power losses due to nonlinear phenomena are not included in the simulation, either. These power losses are proportional to the pressure amplitude in multi-stage looped TAEG. Evidence of the acoustic power loss in the experiment is that a temperature of about 70 °C has been detected on the walls of RTs caused by the waste heat converted from the acoustic power loss.

According to Fig. 24(b), the influence of the length of RTs on thermoacoustic efficiency is limited. With the same electric resistance, the multi-stage looped TAEG with 1.5 m RTs and 2 m RTs almost have the same thermoacoustic efficiency. The thermoacoustic efficiencies in experiment with RTs of 1.5 m are 21.7 %, 22.7 %, 23.1 %, 23 % and 22.8 % with the electric resistance increasing from 40 Ω to 60 Ω, and the thermoacoustic efficiencies in experiment with RTs of 2 m are 21.2 %, 21.6 %, 22.1 %, 22.6 %, 22.9 %, 23.5 %, 23.8 %, and 23.9 % with the electric resistance increasing from 40 Ω to 70 Ω. In the simulation, the thermoacoustic efficiency varies from 30 % to 35 % either with 1.5 m or 2 m RTs, while in the experiment, the thermoacoustic efficiency varies from 20 % to 25 %. The big difference between the simulation and experiment in thermoacoustic efficiency resulted from the fact that much more heat has been input into multi-stage looped TAEG in the experiment than simulation, but less acoustic power is produced. The difference in the heat input between the simulation and experiment is caused by the reasons as follows: 1. Heat leakage through the insulation material: Due to the difficulty in manufacturing progress, the insulation material covering the regenerator and heater block can't be too thick. Therefore, some heat that should be used by the thermoacoustic effect is transferred through the insulation material inevitably. 2. Heat leakage through the stainless wall of the regenerator and thermal buffer tube: Because of the high pressure in the multi-stage looped TAEG, the walls of the regenerator and thermal buffer tube can't be too thin. Thus, some heat should be utilized by the heater block now is conducted through the walls to the main ambient heat exchanger and the second ambient heat exchanger. 3. The second-order mass streaming—Rayleigh streaming, causes the heat that should be used by the thermoacoustic effect, to transfer to the second ambient heat exchanger directly. The heat leakage and the Rayleigh streaming cause more heat consumption in the experiment than in the simulation in which no heat leakage and Rayleigh streaming are assumed. The reason that less acoustic power is produced in the experiment than in the simulation has been stated in the last paragraph. All the reasons mentioned above result in the difference in thermoacoustic efficiency between the simulation and experiment.

Fig. 25 shows the thermal-to-electric conversion characteristics of multi-stage looped TAEG. Fig. 25(a) shows the acoustic-to-electric efficiency of LA with RTs of 1.5 m and 2 m under different electric resistances. Neither the length of RTs nor the electric resistance has an obvious effect on the efficiency. The acoustic-to-electric efficiencies in experiment with RTs of 1.5 m are 73.1 %, 75.1 %, 75.9 %, 77.2 % and 78 % with the electric resistance increasing from 40 Ω to 60 Ω, and the acoustic-to-electric efficiencies in experiment with RTs of 2 m are 74.9 %, 76.7 %, 78.4 %, 79.6 %, 80.6 %, 81.1 %, 81.7 %, and 82.1 % with the electric resistance increasing from 40 Ω to 70 Ω. From Fig. 25(b), we can find that prolonging the length of RTs can increase the output electric power of multi-stage looped TAEG. With the increase of the length of RTs from 1.5 m to 2 m, the maximum output electric power in the experiment increases from 5.1 kW to 6.24 kW. Fig. 25(c) shows the thermal-to-electric efficiency of multi-stage looped TAEG. Like thermoacoustic efficiency, the length of RTs has a limited effect on thermal-to-electric efficiency. The thermoacoustic efficiencies in experiment with RTs of 1.5 m are 15.8 %, 17 %, 17.5 %, 17.7 % and 17.8 % with the electric resistance increasing from 40 Ω to 60 Ω, and the thermoacoustic efficiencies in experiment with RTs of 2 m are 15.9 %, 16.5 %, 17.3 %, 18 %, 18.4 %, 19 %, 19.4 %, and 19.6 % with the electric resistance increasing from 40 Ω to 70 Ω. The overestimation of output electric power and thermal-to-electric efficiency in simulation mainly results from the underestimation of acoustic power loss and heat consumption in simulation, which has been mentioned in the last paragraph.

5. Conclusion

The influence of the length of RTs on multi-stage looped TAEG is numerical and experimental studied in this paper. A 3-step multi-stage looped TAHE and LA coupling method is thoroughly introduced and used in the numerical study. In the experiment, two sets of RTs with lengths of 1.5 m and 2 m are installed. With the increase of the length of RTs from 1.5 m to 2 m, the frequency decreases from 70 Hz to 62 Hz. The maximum output acoustic power increases from 6.97 kW to 8.16 kW, and the maximum output electric power increases from 5.1 kW to 6.24 kW. Meanwhile, the maximum thermoacoustic efficiency increases from 23.08 % to 23.94 %, the maximum acoustic-to-electric efficiency

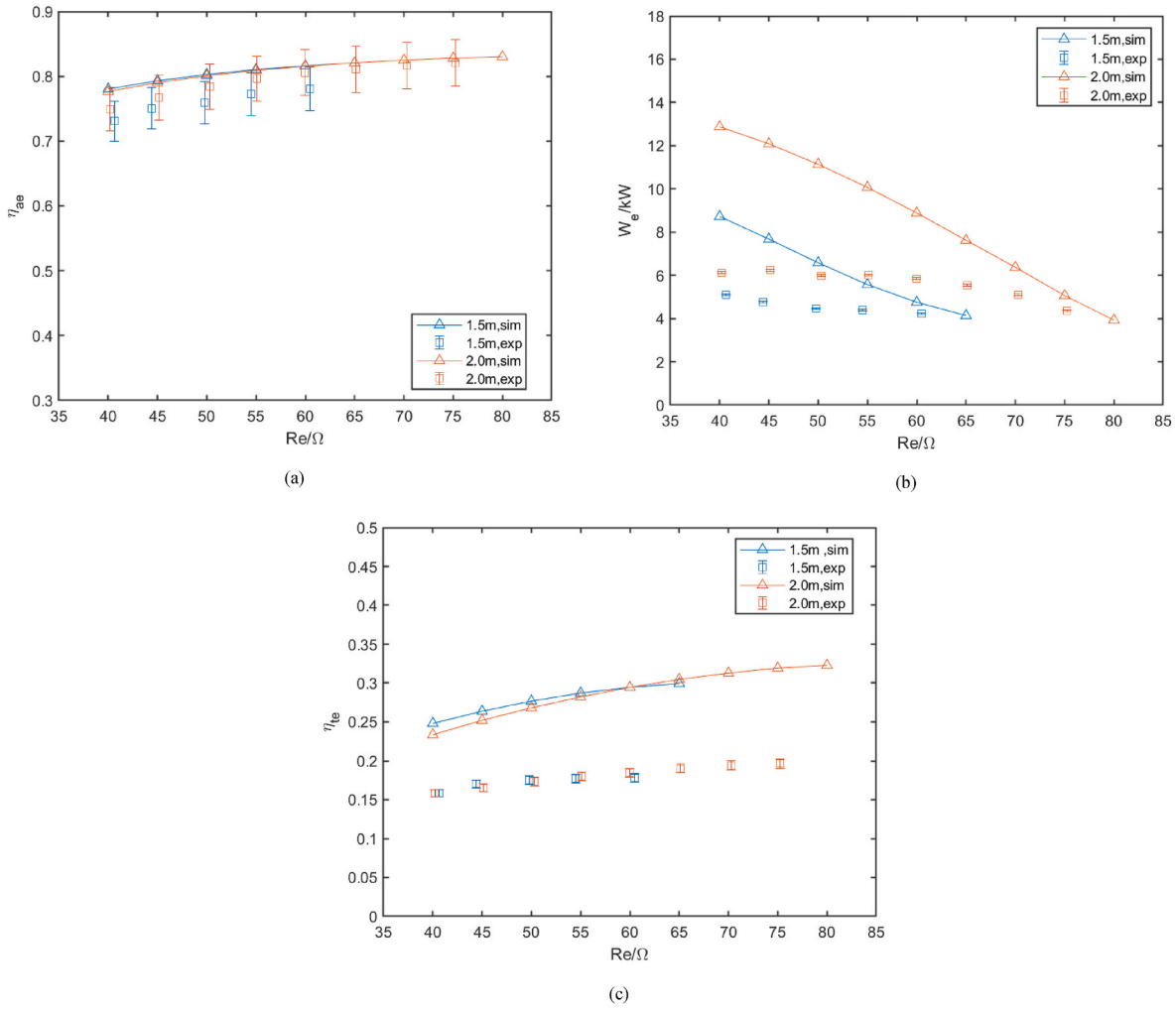

Fig. 25. (a) Acoustic-to-electric efficiency (η_{ae}) (b) output electric power (W_e) and (c) thermal-to-electric efficiency (η_{te}) of multi-stage looped TAEG with RTs of 1.5 m and 2 m under different load electric resistances (Re) (sim: simulation, exp: experiment, TAEG: thermoacoustic electric generator, RT: resonance tube).

increases from 78.03 % to 82.06 % and the maximum thermal-to-electric efficiency increases from 17.79 % to 19.64 %. The simulation results are consistent with the variation trend. This study demonstrates that adjusting the length of RTs is an effective way to tune the frequency of multi-stage looped TAEG and improve the coupling between the multi-stage looped TAHE and LA.

CRediT authorship contribution statement

Tianjiao Bi: Formal analysis, Investigation, Software, Writing – original draft. **Zhanghua Wu:** Conceptualization, Investigation, Software, Writing – review & editing. **Limin Zhang:** Methodology, Software. **Jingyuan Xu:** Conceptualization, Writing – review & editing. **Ercang Luo:** Conceptualization, Supervision, Writing – review & editing. **Chao Li:** Writing – review & editing. **Bin Zhang:** Writing – review & editing. **Wei Chen:** Writing – review & editing.

Declaration of competing interest

The authors declare that they have no known competing financial interests or personal relationships that could have appeared to influence the work reported in this paper.

Data availability

No data was used for the research described in the article.

Acknowledgements

This work is financially supported by the Natural Science Foundation of Shandong Province (Grant No. ZR2020ME172).

Appendix. Acoustic-mechanical-electrical coupling equivalent circuit model of dual opposed LA [12]

In this appendix, the acoustic-mechanical-electrical coupling equivalent circuit model of dual-opposed LA is briefly introduced. Fig. 26 shows the detailed schematic of dual-opposed LA, the meanings of symbols in the figure are tabulated in Table 2.

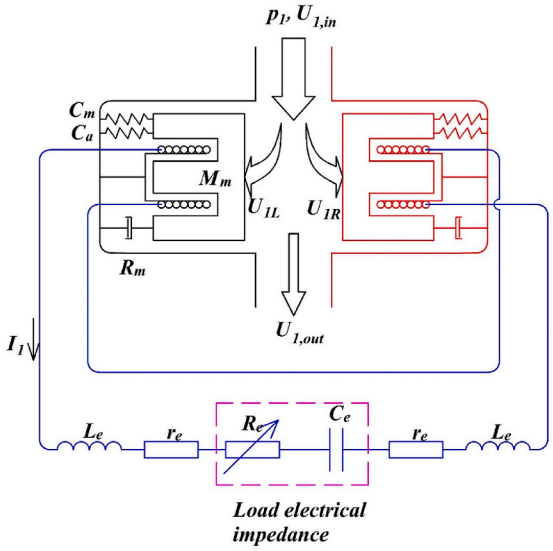

Fig. 26. Detailed schematic of dual-opposed LA.

Table 2
The meanings of the symbols in Fig. 26

Symbol	Meaning	Symbol	Meaning
p_1	Oscillating pressure of acoustic wave	M_m	Mass of piston (piston diameter: D, magnetic induction: B)
$U_{1,in}$	Oscillating volume velocity of acoustic wave	R_m	Mechanical resistance caused by the friction of the piston
U_{1L}	Oscillating volume velocity flows into the left single motor	I_1	Current in the electrical circuit
U_{1R}	Oscillating volume velocity flows into the right single motor	L_e	Electrical inductance of fixed coil
$U_{1,out}$	Oscillating volume velocity flows into the next stage	r_e	Electrical resistance of fixed coil
C_m	Mechanical compliance of flexure bearing connected to the piston	R_e	Load electrical resistance
C_a	Effective acoustic compliance of the gas spring in the back cavity of LA	C_e	Load electrical capacitance

Fig. 27(a) shows the equivalent circuit of acoustic, mechanical and electrical parts of dual-opposed LA each in their respective domains. The acoustic domain and mechanical domain are linked by a transformer with a ratio of *1:S*, due to the relationship of driving source p_1 and F_1 is $p_1/F_1=1/S$. The mechanical domain and electrical domain are linked by a transformer with a ratio of *BL:1* due to the relationship of Ampere's force and the electrical current I_1 of a coil with length L in a magnetic induction B is $F_1=I_1BL$.

The equivalent circuit of dual-opposed LA with all elements converted to mechanical impedance domain is shown in Fig. 27(b), in which $X_m=\omega M_m 1/\omega C_m$ and $R_{et}=R_e+2r_e$. u_1~u_3 mean the mesh currents. After applying the superposition theorem to the equivalent circuit in Fig. 27(b), which retains only one independent driving force source and turns off the other, two equivalent circuits can be obtained as shown in Fig. 27(c) and (d). The velocity of the circuit is determined by the contribution of each of the driving force sources and adding them up, i.e., $u_1=v_1+w_1$, $u_2=v_2+w_2$ et al. For Fi g. 27(c), applying Kirchhoff voltage laws (KVL) to the 3 circuit meshes, we can obtain

$$\begin{cases} F_1+(R_m+iX_m)v_1+\dfrac{(BL)^2}{R_{et}}(v_1 \quad v_2)+\dfrac{S^2}{i\omega C_a}v_1=0 \\ \dfrac{(BL)^2}{R_{et}}(v_2 \quad v_1)+\dfrac{(BL)^2}{iX_e}(v_2 \quad v_3)=0 \\ \dfrac{(BL)^2}{iX_e}(v_3 \quad v_2)+(R_m+iX_m)v_3+\dfrac{S^2}{i\omega C_a}v_3=0 \end{cases} \tag{A.1}$$

For Fig. 27(d), we can obtain

$$\begin{cases} (R_m+iX_m)w_1+\dfrac{(BL)^2}{R_{et}}(w_1 \quad w_2)+\dfrac{S^2}{i\omega C_a}w_1=0 \\ \dfrac{(BL)^2}{R_{et}}(w_2 \quad w_1)+\dfrac{(BL)^2}{iX_e}(w_2 \quad w_3)=0 \\ \dfrac{(BL)^2}{iX_e}(w_3 \quad w_2)+(R_m+iX_m)w_3+F_1+\dfrac{S^2}{i\omega C_a}w_3=0 \end{cases} \tag{A.2}$$

Fig. 27

(a) The equivalent circuit of LA with the acoustic, mechanical and electrical parts each in their respective domains (b) Converting all the elements to mechanical-impedance domain through their transformers respectively (c) and (d) are the equivalent circuits with only one driving force source and the other turned off

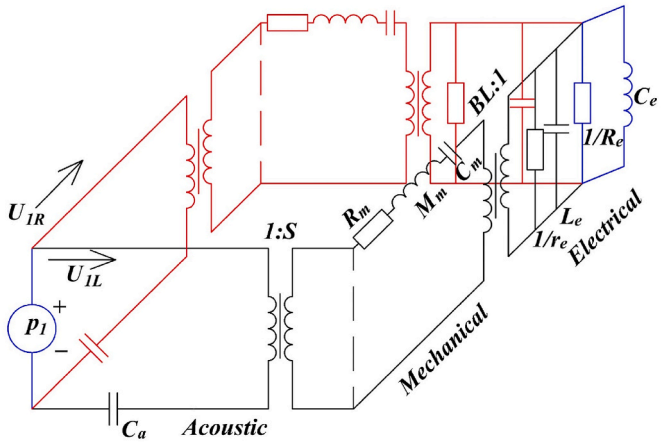

(a)

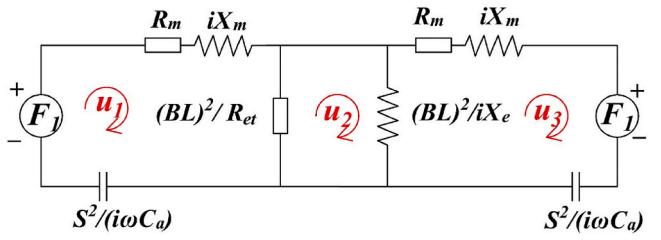

(b)

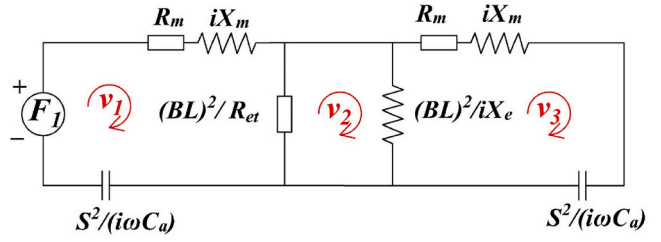

(c)

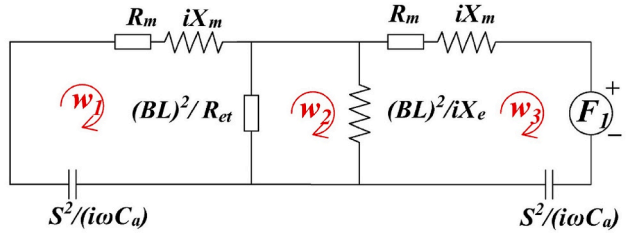

(d)

These two liner equation systems have three unknown variables and three equations. The Gauss elimination method can be used to solve the equations using MATLAB software.

The time-averaged input acoustic power due to the gas oscillation in the front cavity is

$$W_a = \overline{F_1 \cdot u_1} + \overline{F_1 \cdot u_3} = \frac{1}{2}\mathrm{Re}[F_1 \tilde{u}_3] + \frac{1}{2}\mathrm{Re}[F_1 \tilde{u}_3] \tag{A.3}$$

The time-averaged output electric power is

$$W_e = \overline{F_{Re} \cdot u_{Re}} = \frac{1}{2}|u_1 \quad u_2|^2 \cdot \frac{(BL)^2}{R_{et}} \cdot \frac{R_e}{R_{et}} \tag{A.4}$$

The acoustic-to-electric efficiency of the LA is

$$\eta_{ae} = \frac{W_e}{W_a} \tag{A.5}$$

References

[1] Rott N. In: Yih C-S, editor. Thermoacoustics *Advances in Applied Mechanics* vol 20. Elsevier; 1980. p. 135–75.

[2] Chen G, Tang L, Mace B, Yu Z. Multi-physics coupling in thermoacoustic devices. A review Renewable and Sustainable Energy Reviews 2021;146:111170.

[3] Kisha W, Riley P, McKechnie J, Hann D. Asymmetrically heated multi-stage travelling-wave thermoacoustic electricity generator *Energy*, vol. 235; 2021, 121312.

[4] Bahrami M, Ommi F. Performance of a multi-stage thermoacoustically-driven pulse tube cryocooler: Uncertainty quantification and sensitivity analysis. Appl Therm Eng 2022;200:117653.

[5] Yang R, Blanc N, Ramon GZ. Theoretical performance characteristics of a travelling-wave phase-change thermoacoustic heat pump *Energy Conversion and Management* 2022;254:115202.

[6] de Blok K 2010 5.5.5 Novel 4-stage traveling wave thermoacoustic power generator *ASME 2010 3rd Joint US-European Fluids Engineering summer Meeting: volume 2, Fora* ASME 2010 3rd Joint US-European Fluids Engineering summer Meeting collocated with 8th International Conference on Nanochannels, Microchannels, and Minichannels (Montreal, Quebec, Canada: ASMEDC) pp 73–79.

[7] Yang R, Wang Y, Luo J, Tan J, Jin T. Performance comparison of looped thermoacoustic electric generators with various thermoacoustic stages. Int J Energy Res 2020;44:1103–12.

[8] Xu J, Hu J, Sun Y, Wang H, Wu Z, Hu J, Hochgreb S, Luo E. A cascade-looped thermoacoustic driven cryocooler with different-diameter resonance tubes. Part II: experimental study and comparison *Energy* 2020;207:118232.

[9] Xu J, Luo E, Hochgreb S. A thermoacoustic combined cooling, heating, and power (CCHP) system for waste heat and LNG cold energy recovery *Energy*, vol. 227; 2021, 120341.

[10] Jin T, Yang R, Wang Y, Feng Y, Tang K. Low temperature difference thermoacoustic prime mover with asymmetric multi-stage loop configuration. Sci Rep 2017;7:7665.

[11] Bi T, Wu Z, Zhang L, Yu G, Luo E, Dai W. Development of a 5 kW traveling-wave thermoacoustic electric generator. Appl Energy 2017;185:1355–61.

[12] Bi T, Wu Z, Chen W, Zhang L, Luo E, Zhang B. Numerical and experimental research on a high-power 4-stage looped travelling-wave thermoacoustic electric generator. Energy 2022;239:122131.

[13] Hamood A, Jaworski AJ, Mao X, Simpson K. Design and construction of a two-stage thermoacoustic electricity generator with push-pull linear alternator. Energy 2018; 144:61–72.

[14] Al-Kayiem A, Yu Z. Numerical investigation of a looped-tube traveling-wave thermoacoustic generator with a bypass pipe. Energy Proc 2017;142:1474–81.

[15] Hamood A, Jaworski AJ, Mao X. Development and assessment of two-stage thermoacoustic electricity generator *energies*, vol. 12; 2019. p. 1790.

[16] Kruse A, Ruziewicz A, Nemś A, Tajmar M. Numerical analysis of competing methods for acoustic field adjustment in a looped-tube thermoacoustic engine with a single stage. Energy Convers Manag 2019;181:26–35.

[17] Xu J, Hu J, Luo E, Zhang L, Dai W. A cascade-looped thermoacoustic driven cryocooler with different-diameter resonance tubes. Part I: theoretical analysis of thermodynamic performance and characteristics. Energy 2019;181:943–53.

[18] Xu J, Hu J, Sun Y, Wang H, Wu Z, Hu J, Hochgreb S, Luo E. A cascade-looped thermoacoustic driven cryocooler with different-diameter resonance tubes. Part II: experimental study and comparison *Energy* 2020;207:118232.

[19] Wang K, Sun D, Zhang J, Xu Y, Luo K, Zhang N, Zou J, Qiu L. An acoustically matched traveling-wave thermoacoustic generator achieving 750 W electric power. Energy 2016;103:313–21.

[20] Gedeon D. DC gas flows in stirling and pulse tube cryocoolers *cryocoolers 9* ed R G ross. Boston, MA: Springer US; 1997. p. 385–92.

[21] Ward B, Clark John P, Swift Gregory W. Design environment for low-amplitude thermoacoustic energy conversion, DeltaEC Version 6.4 b2 Users Guide. Los Alamos National Laboratory; 2016 (US, https://www.lanl.gov/org/ddste/aldps/materials-physics-applications/condensed-matter-magnet-science/thermoacoustics/_assets/docs/UsersGuide.pdf.